





Cdc42-Borg4-Septin7 axis regulates HSC polarity and function

Ravinder Kandi^{1,†}, Katharina Senger^{1,†}, Ani Grigoryan¹ , Karin Soller¹, Vadim Sakk¹, Tanja Schuster¹, Karina Eiwien¹, Manoj B Menon^{2,3} , Matthias Gaestel² , Yi Zheng⁴, Maria Carolina Florian^{1,‡}  & Hartmut Geiger^{1,*} 

Abstract

Aging of hematopoietic stem cells (HSCs) is caused by the elevated activity of the small RhoGTPase Cdc42 and an apolar distribution of proteins. Mechanisms by which Cdc42 activity controls polarity of HSCs are not known. Binder of RhoGTPases proteins (Borgs) are known effector proteins of Cdc42 that are able to regulate the cytoskeletal Septin network. Here, we show that Cdc42 interacts with Borg4, which in turn interacts with Septin7 to regulate the polar distribution of Cdc42, Borg4, and Septin7 within HSCs. Genetic deletion of either *Borg4* or *Septin7* results in a reduced frequency of HSCs polar for Cdc42 or Borg4 or Septin7, a reduced engraftment potential and decreased lymphoid-primed multipotent progenitor (LMPP) frequency in the bone marrow. Taken together, our data identify a Cdc42-Borg4-Septin7 axis essential for the maintenance of polarity within HSCs and for HSC function and provide a rationale for further investigating the role of Borgs and Septins in the regulation of compartmentalization within stem cells.

Keywords Borg4; Cdc42; HSCs; polarity; Septin7

Subject Categories Cell Adhesion, Polarity & Cytoskeleton; Signal Transduction; Stem Cells & Regenerative Medicine

DOI 10.15252/embr.202152931 | Received 25 March 2021 | Revised 13

September 2021 | Accepted 17 September 2021 | Published online 18 October 2021

EMBO Reports (2021) 22: e52931

Introduction

The function of hematopoietic stem cells (HSCs) decreases upon aging. This contributes, among others, to aging-associated immune remodeling (AAIR) with a reduced production of lymphoid cells (B cells and T cells) and erythroid cells in bone marrow (BM) as well as an increased myeloid output linked to aging-related myeloid

malignancies (Rossi *et al*, 2008; Beerman *et al*, 2010; Geiger *et al*, 2013; Snoeck, 2013; Akunuru & Geiger, 2016). A prominent aging-related phenotype of aged HSCs is a reduced frequency of HSCs with a polar distribution of polarity proteins like Cdc42 or the cytoskeletal protein tubulin or the epigenetic marker histone 4 acetylated on lysine 16 (H4K16ac; Florian *et al*, 2012). Polarity within HSCs is tightly linked to the mode of symmetrical or asymmetrical division. Young (polar) HSCs divide more asymmetrically, while aged (apolar) HSCs divide more symmetrically (Florian *et al*, 2018). The aging-related changes in HSCs and hematopoiesis are caused by both cell intrinsic alterations in HSCs and extrinsic BM niche factors (Kamminga & de Haan, 2006; Geiger *et al*, 2007; Wang *et al*, 2011; Guidi *et al*, 2017; Saçma *et al*, 2019; Mejia-Ramirez & Florian, 2020). An increase in the activity of the small RhoGTPase Cdc42 in aged HSCs causes the reduced frequency of polar HSCs upon aging and is also causative for HSC aging (Florian *et al*, 2012; Grigoryan *et al*, 2018; Leins *et al*, 2018; Liu *et al*, 2019; Amoah *et al*, 2021). Pharmacological attenuation of the aging-related increase in the activity of Cdc42 by a specific small molecule inhibitor of Cdc42 activity termed CASIN resets the frequency of polar HSCs back to level reported for young HSCs and rejuvenates the function of chronologically aged HSC. Cdc42 activity is thus a critical regulator of HSC polarity and aging (Florian *et al*, 2020). While there is information on polarity regulation pathways orchestrated by Cdc42 activity in yeast (Okada *et al*, 2013; Chollet *et al*, 2020), the mechanisms by which Cdc42 controls polarity and especially how elevated activity of Cdc42 results in loss of polarity in HSCs are not understood.

Ectopic expression of either a constitutively active form of Cdc42 or a dominant negative form of Cdc42 leads to redistribution of the borg family of Cdc42 effector proteins (also called Cdc42ep1-5) and subsequent loss of Septin filaments in cell lines (Joberty *et al*, 2001; Farrugia & Calvo, 2017). Septins are GTP-binding proteins that interact in stable stoichiometry within each other to form filaments that bind to the cell membrane, actin filaments, and microtubules. Septins are regarded as the fourth

1 Institute of Molecular Medicine, Ulm University, Ulm, Germany

2 Institute of Cell Biochemistry, Hannover Medical School, Hannover, Germany

3 Kusuma School of Biological Sciences, Indian Institute of Technology Delhi, New Delhi, India

4 Division of Experimental Hematology and Cancer Biology, Cincinnati Children's Hospital Medical Center, Cincinnati, OH, USA

*Corresponding author. Tel: +49 731 50 26700; Fax: +49 731 50 26710; E-mail: hartmut.geiger@uni-ulm.de

†These authors contributed equally to this work

‡Present address: Program of Regenerative Medicine, IDIBELL, Barcelona, Spain

component of the cytoskeleton (Mostowy & Cossart, 2012). In yeast, Septins are recruited to the site of polarization by active Cdc42 while at the same time inhibiting Cdc42 activity in a negative feedback loop (Okada *et al*, 2013). In budding yeast *gic1*, a functional homologue of mammalian Borg proteins, binds to *cdc42*-GTP which in turn leads to dissociation of *gic1* from Septin filaments (Brown *et al*, 1997; Sadian *et al*, 2013, 1). Septins have gained recently more attention, also with respect to the hematopoietic system, like we and others have reported distinct roles for Septin6 (Senger *et al*, 2017) and Septin1 (Ni *et al*, 2019) in hematopoiesis, while the borg family of Cdc42 effector proteins still remains largely uncharacterized, particularly within the hematopoietic system. Here, we demonstrate that a Cdc42-Borg4-Septin7 axis regulates the intracellular distribution of polarity proteins in HSCs in response to changes in Cdc42 activity. Consequently, either Borg4 or Septin7 is critical for HSC function upon stress. Our results provide a novel scientific rationale for a role of Borgs and Septins in the compartmentalization of components within stem cells likely to be essential for stem cell function.

Results

Borg4 and Septin7 show a polar distribution in HSCs, which is regulated by Cdc42 activity

There are 5 known distinct binders of Rho GTPases proteins (Borgs), also known as Cdc42ep4 1-5, which can serve as Cdc42 effector proteins. Borgs are able to bind septins via a conserved BD3 domain and interact with Cdc42 through a Cdc42/Rac interactive binding (CRIB) motif. Borgs play an important role in cytoskeletal rearrangement. They also regulate cell shape, filopodia formation, and cell migration and which are controlled by specific interaction with active Cdc42-GTP (Farrugia & Calvo, 2016). We first determined the level of expression of Borgs in HSCs. *Borgs2-4* were expressed in LT-HSCs (Lin, c-Kit⁺, Sca-1⁺, flk2⁻, CD34⁻ cells) (Fig 1A), whereas *Borgs1* and 5 were absent or below the level of detection (Appendix Table S2). Expression of *Borg2* and 3 was increased and *Borg4* was decreased in aged (elevated level of Cdc42 activity) compared to young LT-HSCs. There are 13 distinct mammalian Septins. *Septin2*, 6, 7, 8, 9, 10, or 11 are thought to be

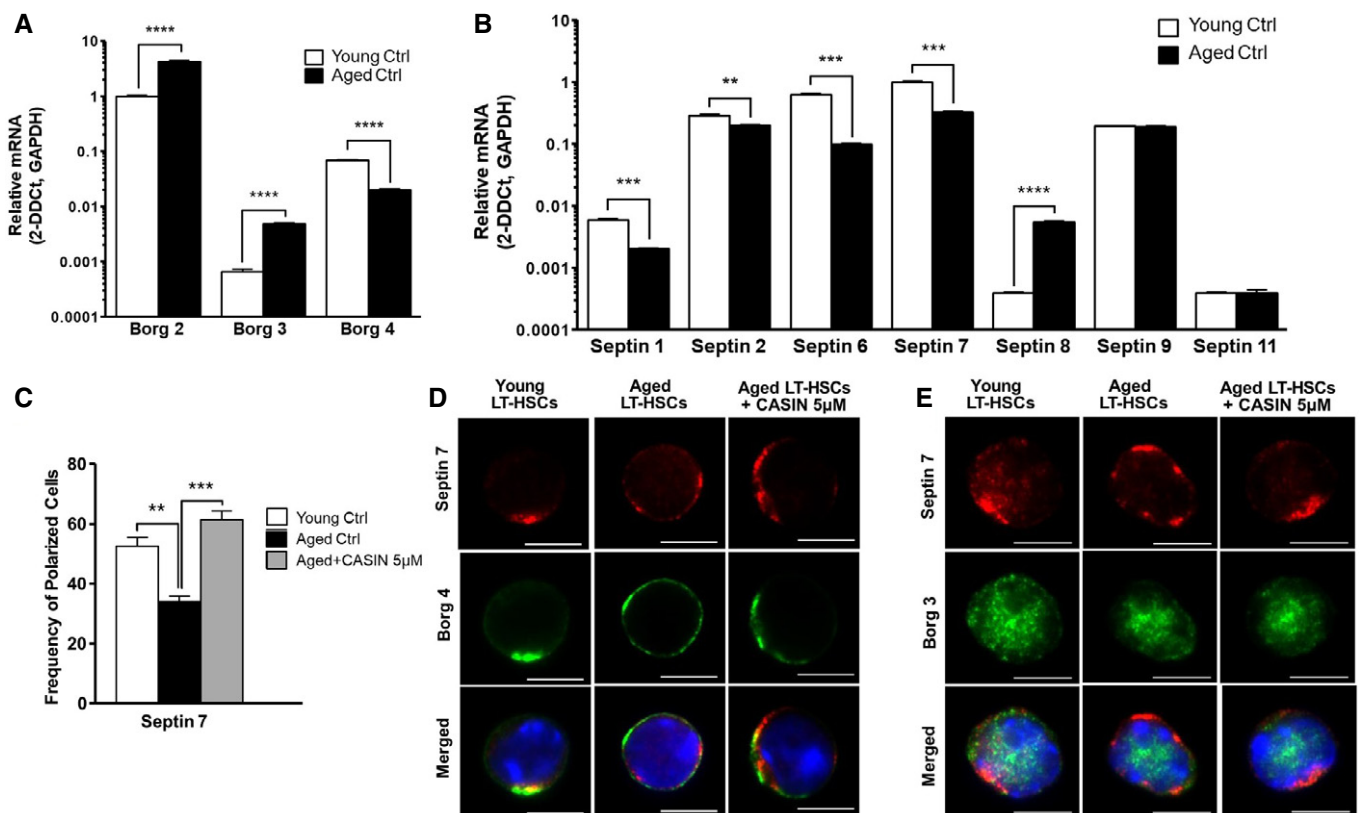


Figure 1. Borg4 and Septin7 show a polar distribution in HSCs which is regulated by Cdc42 activity.

- A, B Level of expression of *Borgs* and *Septins* in young and aged LT-HSCs. mRNA levels of *Borgs* and *Septins* were normalized to the level of expression of *GAPDH* and *Borgs* are shown relative to the level of *Borg2* expression in young LT-HSCs. *Septins* are shown relative to the level of *Septin7* expression in young LT-HSCs. At least three biological replicates ($n = 3$) are shown. Error bars indicate mean \pm SEM, unpaired *t*-test, $**P < 0.01$, $***P < 0.001$, $****P < 0.0001$.
- C Percentage of cells polarized for Septin7 among young, aged, and aged LT-HSCs treated with CASIN (5 μ M). At least 3 biological repeats, at least 50 cells were scored per sample. Error bars indicate mean \pm SEM, unpaired *t*-test, $**P < 0.01$, $***P < 0.001$.
- D, E Representative immunofluorescence microscopy images of the distribution of Septin7 (red) or Borg3 or Borg4 (green) in young, aged, and aged LT-HSCs treated with CASIN (5 μ M). Nuclei were stained with DAPI (blue), scale bar = 5 μ m.

ubiquitously expressed, while expression of *Septin1*, 3, 4, 5, 12, or 14 is usually restricted to distinct tissues or cell types. *Septin1*, 2, 6, 7, 8, 9, and 11 were indeed expressed in LT-HSC, while *Septin3*, 4, 5, 10, 12, and 14 were absent or below the level of detection (Appendix Table S1 and S2). The expression of *Septin1*, 2, 6, and 7 was decreased in aged LT-HSCs, while expression of *Septin8* was increased upon aging (Fig 1B). The level of expression of *Septin9* and 11 was similar in young and aged LT-HSCs. In summary, a distinct set of borgs and septins are expressed in LT-HSCs, and most borgs and septins that are expressed in HSCs show changes in expression in aged compared to young HSCs. Expression data on *Septins* and *Borgs* in murine HSCs and hematopoiesis from public data sets (bloodspot, <https://servers.binf.ku.dk/bloodspot/>, Figs EV2A–M and EV3A–F) are in general consistent with our expression data (Chambers *et al*, 2007).

Septins function in a physiological manner to align with scaffolds (tubulin, actin, and vimentin) to allow for compartmentalization. In yeast, Septins control the diffusion of specific proteins between mother and bud cells, regulating cellular aging (Takizawa *et al*, 2000; Shcheprova *et al*, 2008). We therefore investigated whether the spatial distribution of Septin proteins is distinct in young and aged LT-HSCs using immunofluorescence analyses, and if so, whether changes in the distribution are a consequence of the elevated level of Cdc42 activity in aged LT-HSCs. The core Septin filament structure consists of Septin2, 6, and 7 (Low & Macara, 2006; Sirajuddin *et al*, 2007). We therefore focused first on the localization of Septin2, 6, and 7 in HSCs. The distribution of Septin7 was polarized in about 50% of young but only in about 30% of aged LT-HSCs (Figs 1C and D, and EV10), while only a very low frequency of LT-HSC (young or aged) were polar for either Septin2 or Septin6 (Fig EV1K–M).

Aged HSCs possess an elevated activity of Cdc42 (more Cdc42-GTP) in comparison with young HSCs. The level of Cdc42 activity has been shown to control the spatial distribution of Septins via Borg effector proteins in both yeast and mammalian cell lines (Joberty *et al*, 2001). The distribution of Septins in HSCs might therefore be regulated by the interaction of Septins with the Borg family of Cdc42 effector proteins (Sheffield *et al*, 2003; Farrugia & Calvo, 2016). We first tested whether a reduction of the elevated activity of Cdc42 in aged HSCs to the level reported for young HSCs with a specific inhibitor of Cdc42 activity termed CASIN (Florian *et al*, 2012; Grigoryan *et al*, 2018; Leins *et al*, 2018; Liu *et al*, 2019; Amoah *et al*, 2021) might influence distribution of Septin2, 6 or 7 in aged LT-HSCs. Inhibition of Cdc42 activity increased the frequency of aged LT-HSCs polar for Septin7 to the frequency reported for young LT-HSCs (Fig 1C and D) while the distribution of Septin2 and 6 was not affected by CASIN (Fig EV1K–M). We also tested whether Borgs expressed in LT-HSCs and for which antibodies were available (Borg3 (Cdc42ep5) and Borg4 (Cdc42ep4) might show co-distribution with septins. Borg4 co-localized with Septin7 in young and aged, CASIN treated LT-HSCs repolarized for Septin7, but not in aged LT-HSCs (Fig 1D), while Borg3 did not co-localize with Septin7 (Fig 1E). In summary, our data support that the activity of Cdc42 regulates the subcellular compartmentalization of HSCs in very specific and targeted manner, due to the fact that the reduction of Cdc42 activity restored the polarity of Septin7 and Borg4, but not affecting Septin2, 6, and Borg3 distribution.

We also investigated whether the reduction of Cdc42 activity in aged HSCs by CASIN affected the expression of *Septins* and *Borgs* in LT-HSCs to test for a role of Cdc42 activity in regulating the expression of septins and borgs in addition to controlling their distribution. Interestingly, the level of expression *Septin1*, 2, 6, 7, 8, 9, and 11 was increased in CASIN treated aged HSCs, while the expression of septin8 was decreased and thus also more similar to the level in young LT-HSCs (Fig EV1A–G). Similarly, the level of expression of *Borg2* and 4 in aged LT-HSCs was more similar to the level in young LT-HSCs upon reduction of Cdc42 activity by CASIN, while the level of *Borg3* even further increased in aged LT-HSCs upon inhibition of Cdc42 activity (Fig EV1H–J). Analysis of the spatial distribution of Cdc42GTP along with Septin7 and Borg4 identified that these proteins can indeed co-localize in both young and aged LT-HSCs and confirmed an increase in the level of Cdc42-GTP in aged LT-HSCs (Fig EV1N–P). In summary, our data support an influence of Cdc42 activity on the level of expression of distinct *Borgs* and *Septins*, but more importantly on the spatial polar distribution of especially Borg4 and Septin7 in LT-HSCs. Interestingly, Borg4 seems to specifically interact with Cdc42 but not to other small RhoGTPases like RhoA or Rac1 (Joberty *et al*, 1999, 10; Hirsch *et al*, 2001). On the other hand, Septin7 has a particular role in the Septin family due to the fact that it is the only member of its subgroup that cannot be replaced by any other septin in a hexameric or octameric septin assembly (Kremer *et al*, 2005; Tooley *et al*, 2009; Kim *et al*, 2011, 9).

The Cdc42-Borg4-Septin7 interaction in HSCs is regulated by the level of Cdc42 activity

It has been proposed that Cdc42-GTP, but not GDP, binds to borg proteins to ideally position them within the cell while a switch to Cdc42-GDP releases borgs from Cdc42 to allow for interactions with for example Septins to stabilize Septin networks (Farrugia & Calvo, 2016). We tested such a likely direct physical interaction between Cdc42-Borg4 due to their co-distribution in LT-HSCs by a proximity ligation assay (PLA) (Fig 2A). A positive fluorescence signal in a PLA assay indicates a proximity two distinct proteins of at least less than 40 nm between the epitopes which usually equals to physical interaction (Fig EV3G). We observed multiple spots of interactions between Cdc42 and Borg4 in young HSCs, the level of which was elevated in aged LT-HSCs. Aged LT-HSCs in which Cdc42 activity was adjusted by CASIN showed again a level of reduced interaction similar to young LT-HSCs. This implies that the level of Cdc42 activity regulates the level of the Borg4-Cdc42 interaction, with elevated levels of Cdc42-GTP in aged LT-HSCs resulting in enhanced binding of Borg4 to Cdc42 (Fig 2A and B). Similarly, we tested for a physical interaction of Borg4 with Septin7 (Fig 2C and D). There was more interaction in young and aged LT-HSC treated with CASIN, and less in aged LT-HSCs (high Cdc42GTP), implying that Borg4 is indeed more likely to be released from Cdc42GDP to then interact with Septin7 (Fig 2B and D). In case of the Cdc42 and Borg4 interaction, we used Cdc42 knockout cells as a negative control which indeed delivered only minor background signal (Fig EV3 H). The attenuation of the elevated activity of Cdc42 in aged HSCs to the level found in young HSCs regulated the extent of the interaction between Cdc42 and Borg4 and in turn between Borg4 and Septin7. Among the Borgs and Septins expressed in LT-HSCs, Borg4 and Septin7 thus

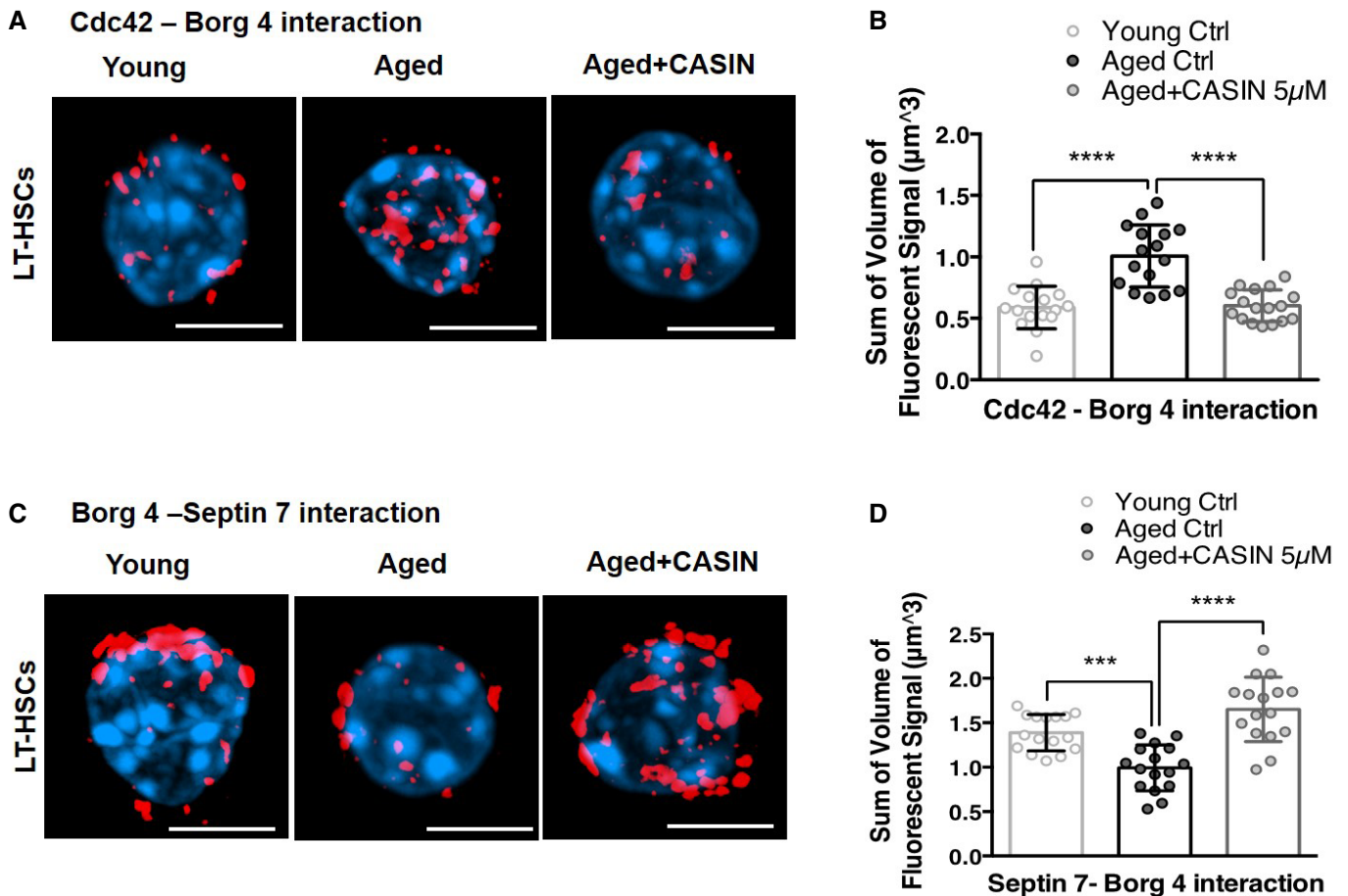


Figure 2. The physical interaction between Cdc42-Borg4-Septin7 is regulated by the activity of Cdc42.

- A Representative immunofluorescence confocal microscopy images of young, aged, and aged + CASIN (5 μM) treated LT-HSCs for the proximity ligation assay (red signal), testing the extent of close physical interaction of Cdc42 and Borg4. A red fluorescent signal indicates close proximity of the two proteins tested. Nuclei were stained with DAPI (blue), scale bar = 5 μm .
- B Quantification of the level of fluorescent signal in young, aged, and aged + CASIN (5 μM) treated LT-HSCs to quantify the Cdc42-Borg4 proximity interaction. Data are normalized to the mean fluorescence signal of aged LT-HSCs. 3 biological repeats, n = at least 17 cells per condition, error bars indicate mean \pm SEM, unpaired t -test, **** P < 0.0001.
- C Representative immunofluorescence confocal microscopy images of young, aged, and aged + CASIN (5 μM) treated LT-HSCs for the proximity ligation assay (red signal), testing the extent of close physical interaction of Borg4 and Septin7. A red fluorescent signal indicates close proximity of the two proteins tested. Nuclei were stained with DAPI (blue), scale bar = 5 μm .
- D Quantification of the level of fluorescent signal in young, aged, and aged + CASIN (5 μM) treated LT-HSCs to quantify the Borg4-Septin7 proximity interaction. Data are normalized to the mean fluorescence signal of aged LT-HSCs. 3 biological repeats, n = at least 17 cells per condition; error bars indicate mean \pm SEM, unpaired t -test, *** P < 0.001, **** P < 0.0001.

specifically build a critical “effector cascade of Cdc42 activity” to confer outcomes on LT-HSCs (like level of the polar distribution of polarity proteins) in response to changes Cdc42 activity in LT-HSCs.

Borg4 or Septin7 regulate the distribution of polarity proteins in HSCs

A general genetic ablation of *Septin7* is embryonic lethal, while general genetic ablation of *Borg4* results in neurological defects (Menon *et al*, 2014; Ageta-Ishihara *et al*, 2015; Abbey *et al*, 2016). To further investigate the role of Borg4 and Septin7 for Cdc42-driven phenotypes like polarity in specifically HSCs and

hematopoietic cells, we used a *vav-1* driven cre-recombinase to delete *Borg4* or *Septin7* in hematopoietic cells of *Borg4^{fllox/fllox}* or *Septin7^{fllox/fllox}* animals (leading to *Borg4^{A/A}* or *Septin7^{A/A}*) (Menon *et al*, 2014; Ageta-Ishihara *et al*, 2015). Deletion of *Borg4* or *Septin7* in hematopoietic cells, including LT-HSCs from *Borg4^{A/A}* or *Septin7^{A/A}* animals, was confirmed by PCR, quantitative RT-PCR or immunofluorescence (Fig EV4A–D). The absence of Borg4 from LT-HSCs resulted in a reduced frequency of LT-HSC polar for the distribution of Septin7 and tubulin but interestingly also for Cdc42 itself (Fig 3A–C), while the frequency of cells polar for the epigenetic polarity marker histone 4 acetylated on lysine 16 (H4K16ac) was only slightly affected by the lack of Borg4

(Fig EV4F and I). The absence of Septin7 from LT-HSCs resulted in a reduced frequency of LT-HSC polar for the distribution of Borg4, tubulin, and, similar to the *borg4^{Δ/Δ}* LT-HSCs, also for Cdc42 (Fig 3D–F) and for H4K16ac (Fig EV4E and H). This implies a feedback loop in which changes in the Septin7 localization and thus likely a disturbed Septin network will in return influence the localization of Cdc42 as well as Borg4. Such a

general feedback loop between Cdc42 localization and Septins has been previously described in yeast (Okada *et al*, 2013) but not yet for stem or even for mammalian cells. Interestingly, the distribution of either Septin2, or Septin6, which are, similar to Septin7, components of the core Septin filament complex, is not affected by a lack of Borg4 (Fig EV4G and J) nor is the distribution of Crumbs3, another marker of polarity in epithelial cells (Fig EV4K

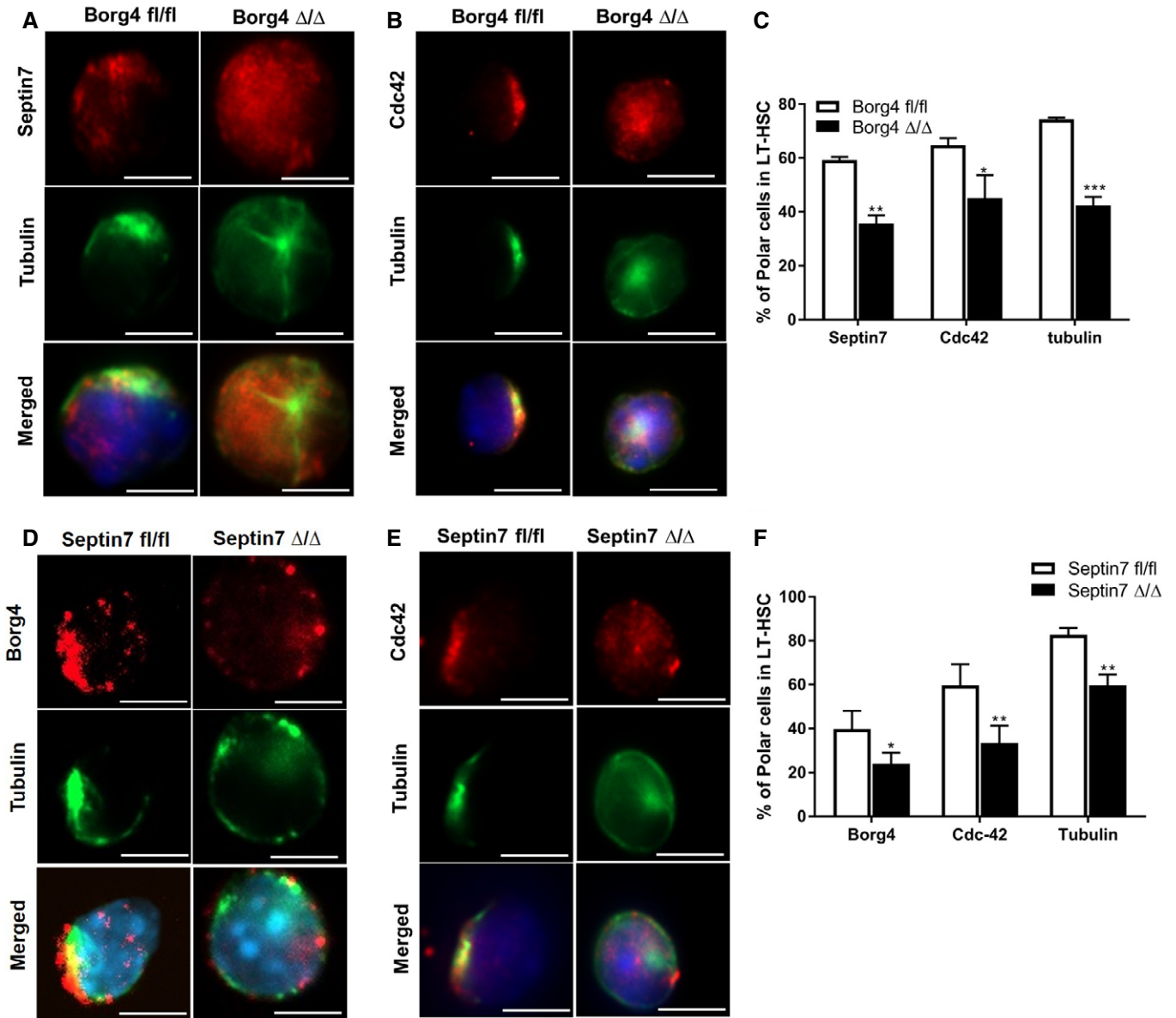


Figure 3. Borg4 or Septin7 regulates the distribution of polarity proteins in HSCs.

A, B Representative immunofluorescence microscopy images of the distribution of Septin7 (red), Cdc42 (red), and tubulin (green) in LT-HSCs from *Borg4^{fl/fl}* or *Borg4^{Δ/Δ}* mice. Nuclei were stained with DAPI (blue), scale bar = 5 μm.
 C Percentage of cells with a polar distribution of Septin7, Cdc42 or tubulin in *Borg4^{fl/fl}* or *borg4^{Δ/Δ}* LT-HSCs. At least 3 biological repeats, at least 50 cells were scored per sample. Error bars indicate mean ± SEM, two-way ANOVA, ****P* < 0.001, ***P* < 0.01, **P* < 0.05.
 D, E Representative immunofluorescence microscopy images of the distribution of borg4 (red), Cdc42 (red) or tubulin (green) in LT-HSCs from *Septin7^{fl/fl}* or *Septin7^{Δ/Δ}* mice. Nuclei were stained with DAPI (blue). Scale bar = 5 μm.
 F Percentage of cells with a polar distribution of Borg4, Cdc42 or tubulin in *Septin7^{fl/fl}* or *Septin7^{Δ/Δ}* LT-HSCs. At least 3 biological repeats, at least 30–50 cells were scored per sample. Error bars indicate mean ± SEM, two-way ANOVA, ***P* < 0.01, **P* < 0.05.

and L). This implies that the positions of core complex Septins within HSCs are not synchronized.

HSCs devoid of Borg4 or Septin7 show impaired function upon transplantation

The interconnected role of both Borg4 and Septin7 for polarity maintenance in LT-HSCs predicts similar changes in the function of HSCs devoid of either Borg4 or Septin7 if the level of polarity is linked to HSC function. We performed analyses of the BM at steady state as well upon competitive transplantation/repopulation. In steady state, the frequency of B- and T- and myeloid cells and the frequency of LT- and ST-HSCs and LMPP was similar in *Borg4^{fl/fl}* and *Borg4^{Δ/Δ}* animals (Fig 4A and B, Appendix Fig S1A–H), as well as the frequency of megakaryocyte erythroid progenitors MEPs, common myeloid progenitors (CMPs) and granulocyte macrophage progenitors (GMPs) (Fig EV5A). In contrast, the frequency of common lymphoid progenitor cells (CLPs) was significantly increased in *Borg4^{Δ/Δ}* BM (Figs 4C and EV5B). *Septin7^{Δ/Δ}* animals, similar to *Borg4^{Δ/Δ}* animals, showed frequencies of B-, T-, and myeloid cells in BM similar to *Septin7^{fl/fl}* controls (Fig 4D). *Septin7^{Δ/Δ}* animals further presented with a slightly elevated frequency of ST-HSCs but not LT-HSCs, and a reduced frequency of LMPPs (Figs 4E and EV5C, Appendix Fig S1I). Similar to our findings in *Borg4^{Δ/Δ}* animals, the frequency of CLPs was also increased in *Septin7^{Δ/Δ}* animals (Fig 4F). Next, competitive transplantation/reconstitution experiments with BM cells from fl/fl or Δ/Δ animals were performed, and donor chimerism was analyzed up to 21 weeks post-transplantation (Fig 4G). Donor chimerism supported by *Borg4^{Δ/Δ}* cells in both PB and BM was reduced by about 50% in comparison with chimerism supported by *Borg4^{fl/fl}* cells (Figs 4H and EV5D), and *Septin7^{Δ/Δ}* cells almost failed to establish any level of donor chimerism (Figs 4I and EV5G). *Septin7^{fl/fl}* as well as *Septin7^{Δ/Δ}* LSK cells showed a similar efficiency in homing to the BM (Fig EV5H), which excludes differential homing to the BM as a cause for the very low level of engraftment of *Septin7^{Δ/Δ}* cells. Animals reconstituted with *Borg4^{Δ/Δ}* cells presented with similar frequencies of B-, T- or myeloid cells among donor-derived cells in BM (Figs 4J and EV5E) or stem and progenitor cells among LSK cells (Fig 4K) or MEPs, CMPs, and GMPs in BM (Fig EV5F). There was though a significant increase in the frequency of donor-derived CLPs in animals reconstituted with *Borg4^{Δ/Δ}* cells (Fig 4L) which mirrors the findings in steady-state hematopoiesis in *Borg4^{Δ/Δ}* animals (Fig 4A–C). Recipients of *Septin7^{Δ/Δ}* cells presented with an

increase in the frequency of B220⁺ B cells and a decrease in the frequency of myeloid cells in BM (Fig 4M) alongside an increase in the frequency of donor-derived LT-HSCs and a reduced LMPP frequency (Fig 4N, Appendix Fig S1J). The frequency of donor-derived CLPs was significantly increased in recipients of *Septin7^{Δ/Δ}* cells compared to fl/fl controls (Fig 4O). In summary, these results indicate that in steady state, CLP frequency is elevated in both *Borg4^{Δ/Δ}* and *Septin7^{Δ/Δ}* mice, while in general hematopoiesis is, in the case of lack of Borg4 or, in the case of lack of Septin7, only slightly affected. Upon competitive transplantation, lack of Borg4 and especially Septin7 in HSCs though results in a highly reduced repopulation potential, and in the case of lack of Septin7 also in a skewing of differentiation, with enhanced lymphoid differentiation at the cost of myeloid cells and a higher frequency of LT-HSCs at the cost of the frequency of LMPPs, but similar to steady state, an elevated frequency of CLPs in BM. These data are also consistent with a finding that T-cell specific deletion of Septin7 results in normal T-cell proliferation *in vivo*, and only impaired T-cell proliferation upon ex vivo expansion (Mujal et al, 2016). Both Borg4 and Septin7 are thus necessary for HSC function, especially upon transplantation stress.

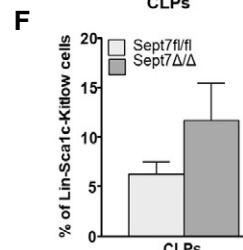
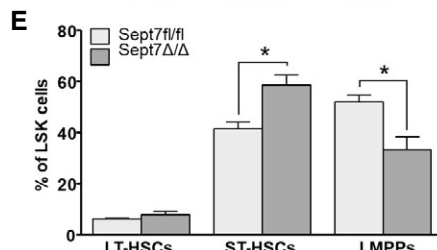
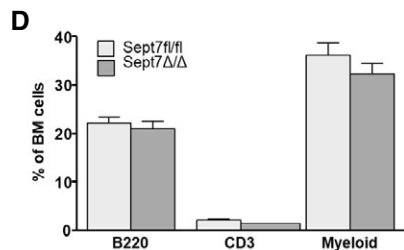
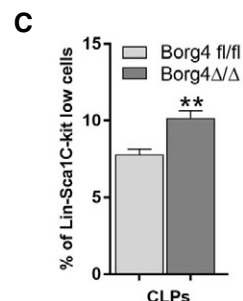
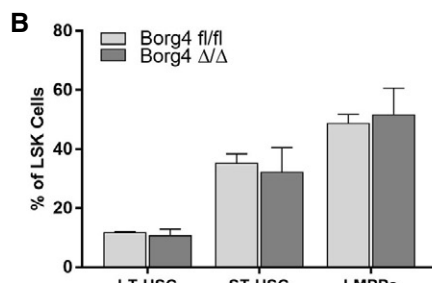
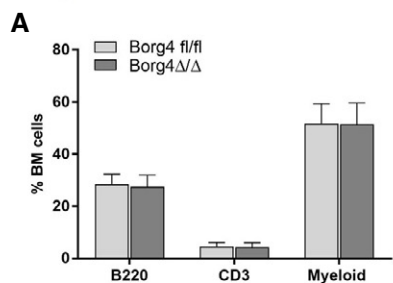
Lack of Septin7 in LT-HSCs impairs HSC proliferation

Lack of Septin7 in HSCs resulted in a severe phenotype upon stress. Septins are known to be essential players in complex processes of compartmentalization, which also include cytokinesis (Kinoshita, 2003). For example, deficiency of Septin7 leads to incomplete cytokinesis in fibroblasts (Menon et al, 2014). We therefore tested whether loss of Septin7 might also influence, in addition to polarity, cell proliferation kinetics of LT-HSCs which might contribute then to graft failure. To test proliferation potential, we determined ex vivo single-cell division kinetics of LT-HSCs. LT-HSCs from *Septin7^{Δ/Δ}* mice completed their first and second division an average later compared to HSCs from control *Septin7^{fl/fl}* mice (Fig 5A). Lack of Septin7 in HSCs also resulted in an increase in the frequency of in LT-HSCs dying in the proliferation culture (Fig 5B). The number of cells generated from individual *Septin7^{Δ/Δ}* HSCs 5 days after initiation of the culture was markedly reduced compared to controls (Fig 5C). While these findings do not support a dramatic role of Septin7 for cytokinesis in HSCs, they imply a role for stem cell survival, but more importantly, indicate a rapid loss of HSC and progenitor potential upon cell division as indicated by the small colony size of individual *Septin7^{Δ/Δ}* HSC.

Figure 4. HSCs devoid of Borg4 or Septin7 show impaired function upon transplantation.

- A–F Percentage of B cells (B220-positive cells), T cells (CD3-positive cells), and myeloid cells (Mac-1⁺ or Gr⁺ positive cells) among BM cells, percentage of LT-HSCs, ST-HSCs, and LMPPs in LSK cells and percentage of CLPs in lin[−]Sca1C-kit low cells in *Borg4^{fl/fl}* or *Borg4^{Δ/Δ}* or *Septin7^{fl/fl}* or *Septin7^{Δ/Δ}* animals at steady state ($n =$ at least 3). Error bars indicate mean \pm SD, * $P < 0.05$, two-way ANOVA, ** $P < 0.01$, unpaired t -test.
- G Experimental setup for competitive bone marrow transplantation experiments.
- H Frequency of donor-derived cells (*Borg4^{fl/fl}* or *Borg4^{Δ/Δ}*) in peripheral blood 4, 8, 16, and 20 weeks post-transplantation ($n = 12$ per group, error bars indicate mean \pm SD, **** $P < 0.0001$, two-way ANOVA).
- I Frequency of donor-derived cells (*Septin7^{fl/fl}* or *Septin7^{Δ/Δ}*) in peripheral blood 8, 16, and 21 weeks post-transplantation ($n = 12$ per group, error bars indicate mean \pm SD, **** $P < 0.0001$, two-way ANOVA).
- J–O Percentage of donor-derived (*Borg4^{fl/fl}* or *Borg4^{Δ/Δ}* or *Septin7^{fl/fl}* or *Septin7^{Δ/Δ}*) B cells (B220-positive cells), T cells (CD3-positive cells), and myeloid cells (Mac-1⁺ or Gr⁺ positive cells) among BM cells, percentage of donor-derived LT-HSCs, ST-HSCs, and LMPPs in LSK cells and percentage of donor-derived CLPs in lin[−]Sca1C-kit low cells in animals at post-transplantation ($n = 12$). Error bars indicate mean \pm SD, **** $P < 0.0001$, ** $P < 0.01$, and * $P < 0.05$, two-way ANOVA and 2-tailed unpaired t -test.

Steady state Bone marrow



Bone marrow Transplantation

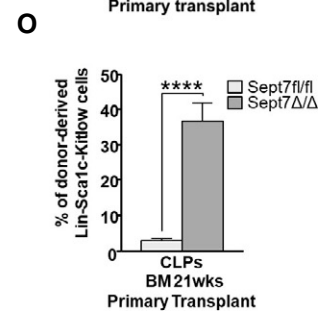
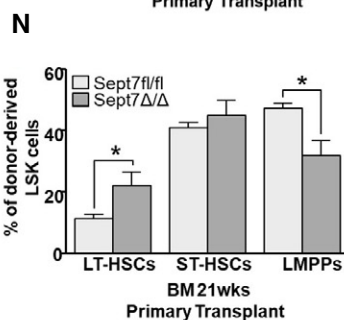
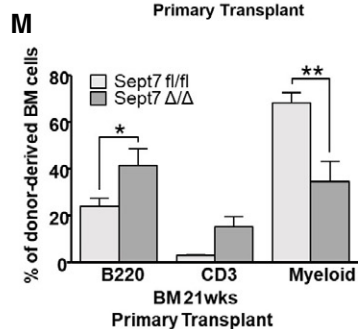
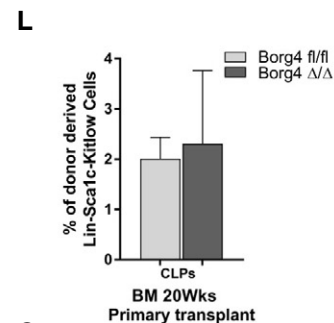
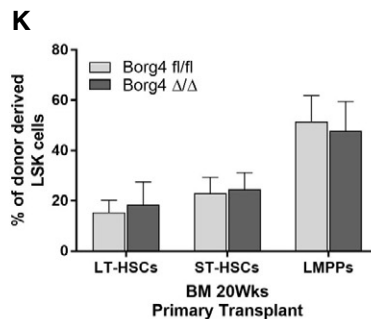
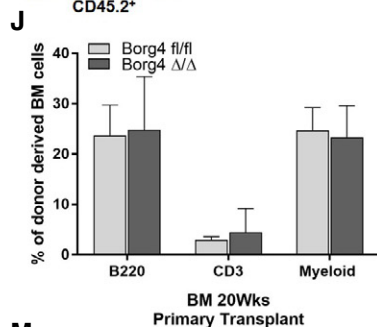
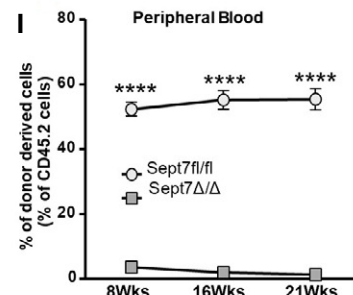
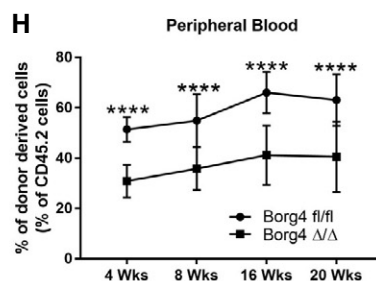
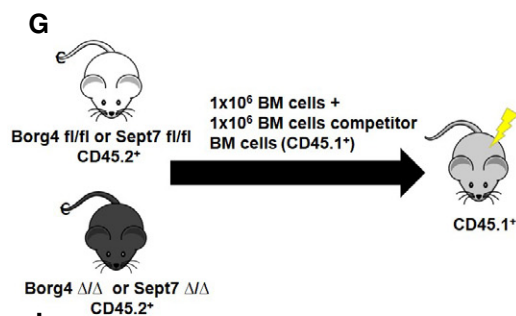


Figure 4.

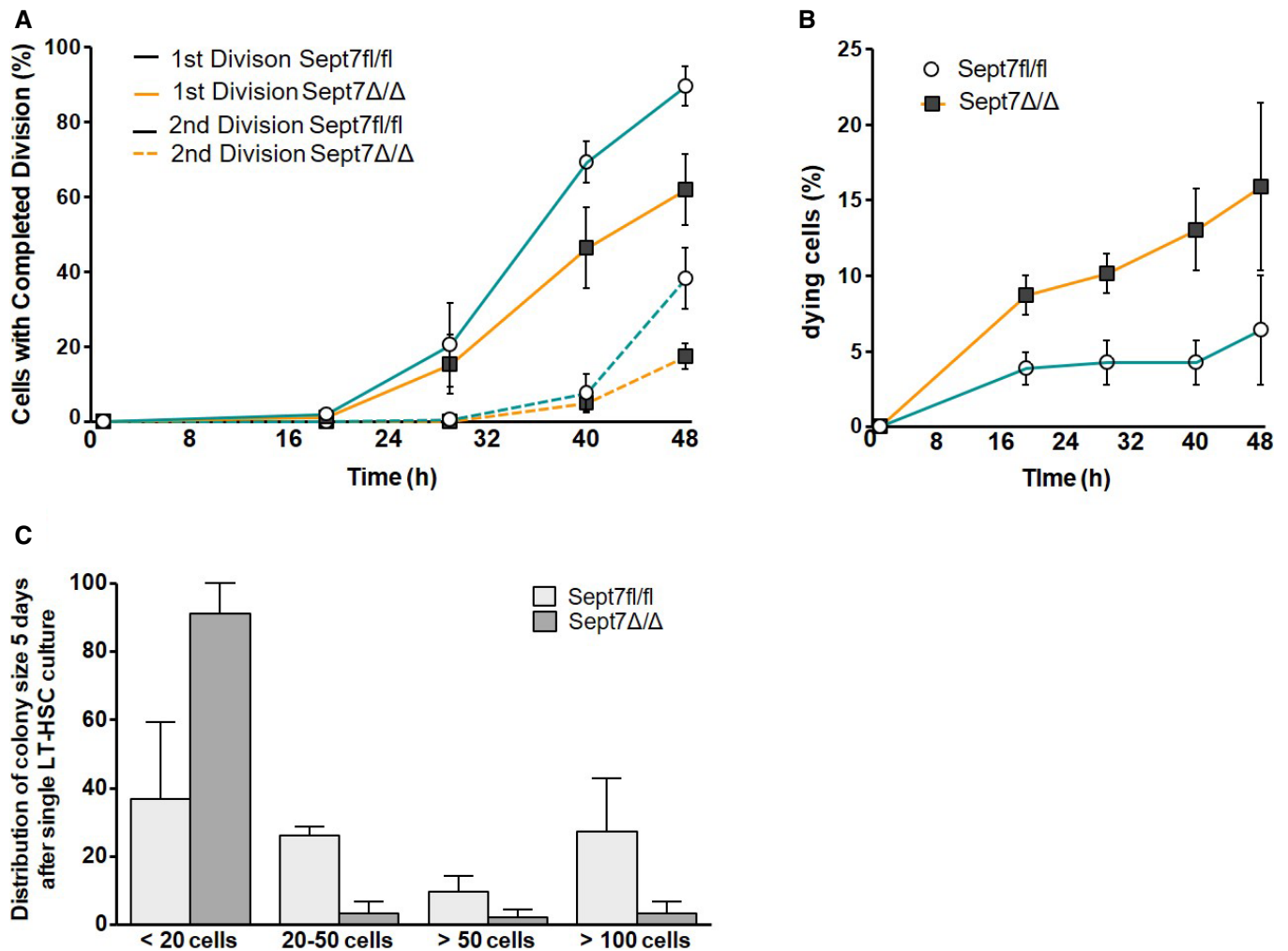


Figure 5. Lack of Septin7 in LT-HSCs impairs HSC proliferation.

- A Percentage of single LT-HSCs from *Septin7^{fl/fl}* or *Septin7^{Δ/Δ}* mice that completed first and second division up to 48 h post-initiation of culture (192 sorted HSC cells were analyzed; error bars indicate mean \pm SD).
- B Percentage of single LT-HSCs *Septin7^{fl/fl}* or *Septin7^{Δ/Δ}* dying up to 48 h (192 sorted HSCs were analyzed; error bars indicate mean \pm SD).
- C Frequency of colonies with distinct cell size 5 days after initiation of culture of individual LT-HSCs from *septin7^{fl/fl}* or *septin7^{Δ/Δ}* mice (192 sorted HSCs were analyzed; error bars indicate mean \pm SD).

Discussion

An increase in the activity of the small RhoGTPase Cdc42 in aged HSCs causes a reduced frequency of polar HSCs and is causative for HSC aging. Polarity within HSCs is tightly linked to the mode of the division. Young (polar) HSCs divide more asymmetrically, while aged (apolar) HSCs divide more symmetrically (Florian *et al.*, 2018). Our published data imply that the PAR polarity complex is likely not linked to polarity regulation in HSCs (Florian *et al.*, 2012), while we assigned a role of osteopontin or Wnt or Yap-Taz-Scribble signaling in regulating Cdc42 activity and Cdc42-induced HSC polarity (Florian *et al.*, 2013; Guidi *et al.*, 2017; Althoff *et al.*, 2020). We further demonstrated that elevated activity of Cdc42 inhibits the expression of lamin A/C in HSCs, and that lack of this nuclear envelop protein induces loss of epipolarity for H4K16ac (Grigoryan *et al.*, 2018;

Mejia-Ramirez & Florian, 2020; Mejia-Ramirez *et al.*, 2020). However, mechanisms by which Cdc42 activity controls polarity within the cytoplasm of HSCs remained so far not well characterized.

Our data demonstrate that an Cdc42-Borg4-Septin7 axis regulates the intracellular distribution of cytoplasmic polarity marker proteins in HSCs in response to changes in Cdc42 activity. Our findings support a model in which Cdc42GTP interacts with Borg4, which is then less likely to interact with Septin7 as it is sequestered at Cdc42GTP (Fig 6). On the other hand, if the activity of Cdc42 is reduced and thus the level of Cdc42GTP reduced, Borg4 binds to Septin7, which stabilizes Septin-7 distribution and by this means likely septin networks to contribute to an orderly compartmentalization within HSCs, as indicated by the elevated frequency of HSCs polar for the distribution of polarity markers.

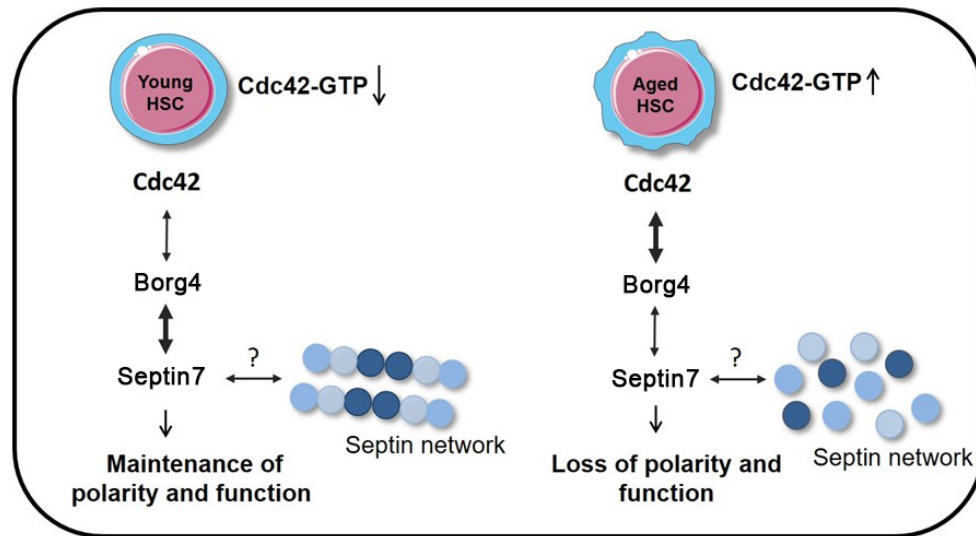


Figure 6. Schematic representation of Cdc42-Borg4-Septin7 axis in the regulation of HSC polarity and function.

It is likely that Borgs and Septins act cell type-specific. Previous studies reported that ectopic expression of active Cdc42 leads, via Borg proteins, to a loss of Septin filament assembly in yeast and mammalian cell lines (Joberty *et al*, 2001). This implies that overall similar mechanisms might be at work in yeast and HSCs, with HSCs though specifically relying on Borg4 and Septin7 to link Cdc42 activity for the regulation of the position of septins. It is likely that this axis is specific for HSCs and that thus other cells or cell types might regulate and use borg-septin interactions differentially, with distinct combinations affecting distinct cytoskeletal/nuclear structures. The data presented in this manuscript are focused on HSCs. The role of specific Borgs and Septins might be distinct in other cell types. For example, Borg3 acts via Septin9 to control actomyosin function and cancer cell invasion (Farrugia *et al*, 2020), and a Cdc42-Borg2-Septin2 axis activates the DNA damage response in cell lines (Eduardo da Silva *et al*, 2020). It remains to be further investigated whether other types of stem cells will rely on a similar axis, or whether distinct types of stem cells will use type-specific combinations of Borgs and Septins to link Cdc42 activity to changes in the septin network.

Changes in HSC polarity are linked to changes in HSC function (Florian *et al*, 2018). Lack of Borg4 or Septin7 in HSCs reduced the frequency of polar HSCs and HSC function was dramatically reduced upon transplantation. It also resulted in an elevated frequency of common lymphoid progenitors (CLPs) in BM while steady-state hematopoiesis was interestingly only marginally affected. Similar changes in the function of HSCs devoid of either Borg4 or Septin7 further support an Cdc42-Borg4-Septin7 axis in HSCs. The data further imply an important inhibitory role of this Borg4-Septin7 axis for the generation of CLPs *in vivo*, by yet unknown mechanisms. The more severe loss of potential of HSCs that lack Septin7 in comparison with lack of Borg4 might be due to the structural role of Septin7 in addition to its regulatory role in HSCs, while Borg4 having primarily a regulatory role. Another possibility is that other Borgs can compensate for the loss of Borg4. This might be less likely as we did for example not detect co-

localization of Borg3 and Septin7 in HSCs (Fig 1E). Although Septin6 is, similar to Septin7, part of the core hexamer complex of Septin filaments, lack of Septin6 increased HSC function as well as the contribution to the B-cell compartment in reconstitution experiments (Senger *et al*, 2017). Together with our finding that core complex septins are not really co-distributed in HSCs (Figs 1D and EV1L and M), there is a possibility that only a small fraction of Septins within HSCs are, in steady state, actually assembled into filament structures, which though will require further investigations. For example, more recently, it was shown that phosphorylation of Septin1 resulted in impaired cytoskeletal remodeling and thus decreased cell rigidity in HSCs (Ni *et al*, 2019).

While lack of for example Cdc42 in HSCs affects hematopoiesis already at steady state, lack of Borg4 or Septin7, effectors of Cdc42 for the regulation of HSC polarity as shown above, affects HSC function primarily upon transplantation. Septin7 is dispensable for the proliferation of B and T cells *in vivo* and in the proliferation of splenocytes and myeloid progenitors *in vitro* (Menon *et al*, 2014; Menon & Gaestel, 2015). Interestingly, it was previously shown that successful proliferation of *Septin7^{A/A}* T cells was strictly dependent cell-to-cell contact (Mujal *et al*, 2016). It is thus a possibility that an altered HSC niche interaction that manifests itself only upon transplantation contributes to the lack of proper function of *Borg4* or *Sept7^{A/A}* HSCs. This hypothesis is consistent with our finding of reduced colony size of HSCs cultivated *ex vivo* without proper niche contact (Fig 5C). More recently, it was also suggested that HSC contributes only marginally to steady-state hematopoiesis, but do so upon transplantation (Busch *et al*, 2015; Dong *et al*, 2020). Another possibility might therefore be that lack of Borg4 or Septin7, and in extension, regulation of polarity, might almost exclusively affect HSCs and only to a minor extent more differentiated cells.

Low level of engraftment potential, reduced frequency of HSCs polar for polarity proteins, increased frequency of LT-HSCs upon transplantation and a decreased frequency of LMPPs found in *Septin7^{A/A}* animals are also hallmarks of aged HSCs (Adolfsson

et al, 2005; Florian *et al*, 2012, 42). On the other hand, *Septin7^{A/A}* HSCs show elevated contribution to lymphoid differentiation and reduced myeloid differentiation that are not seen in aged HSCs. Lack of *Borg4* and *Septin7*, and in extension polarity, thus confer a set of hallmarks of HSC aging. This premature aging phenotype though is only partial or segmental, as for example lymphoid differentiation is rather enhanced in these HSCs.

Additional studies will be necessary to fully elucidate the role of *Cdc42* directed organization of the septin network for the regulation of HSC compartmentalization as well as aging of stem cells.

Materials and Methods

Experimental animals

Young C57BL/6Jrj mice (8–12 weeks old) were obtained from Janvier (France), aged C57BL/6J and C57BL/6.SJL *Ptprc^aPepc^b*/BoyCr1 (BoyJ) mice were derived from the internal divisional stock (based in Charles River Laboratories). *Septin7* knockout mice (C57BL/6J background) have been reported previously (Menon *et al*, 2014). *Borg4* floxed embryos were obtained from RIKEN Bioresource Center, Japan. These embryos were utilized to generate initially *borg4* floxed mice and further to obtain hematopoietic-specific knockout of *Borg4* gene, *Borg4* floxed mice crossed with hematopoietic-specific *Vav1-Cre* transgene containing mice. *Septin7* and *Borg4* mice were confirmed by PCR. The conditional deletion of *Septin7* was tested with primer P1: 5' GGTATAGGGGAC TTTGGGG 3', primer P2: 5' CTTTGCACATATGACTAAGC 3' and primer P3: 5' GCTTCTTTT ATGTAATCCAGG 3' (Menon *et al*, 2014). The *Borg4* conditional deletion was tested with primer a: 5' TGCTTCAGTACCTTCAGGAC 3', primer b: 5' TCGAGTTCACAGAGCTGGA 3' and primer c: 5' TCATAGAGAAGGTGGCAGC 3' (Ageta-Ishihara *et al*, 2015, 42). For the *Vav-Cre* transgene, we used the following primers: Cre-FP 5'CTTCTAGCCTGTACGGAAGTGT3' and Cre-RP 5' CGCGCGCCTGAAGATATAGAAGAT 3' (Croker *et al*, 2004). *Cdc42KO* mice were housed in the Cincinnati Children's Hospital Medical Center (CCHMC) animal facility. All mice were housed under pathogen-free environment in the animal barrier facility at the University of Ulm or at CCHMC. Mouse experiments were performed in compliance with the Laws for Welfare of Laboratory Animals and were approved by the Regierungspräsidentium Tübingen or by the institutional animal care and use committee at CCHMC.

Quantitative real-time PCR

Gene expression analysis was determined by real-time reverse-transcriptase polymerase chain reaction (RT-PCR) as described previously (Senger *et al*, 2017). Briefly, total RNA was extracted from 20,000 LT-HSCs of young and aged C57BL/6J mice as well as aged LT-HSCs treated with 5 μ M CASIN using the RNeasy Micro Kit (Qiagen) according to all manufacturer's instructions. cDNA was prepared and amplified with the Ovation RNA Amplification System V2 (Nu GEN, San Carlos, CA). All real-time polymerase chain reactions were run with Taq MAN Universal PCR Master Mix (Applied Biosystems, Foster City, CA) and with primers from Applied Biosystems on a 7900 HT Fast Real-Time PCR system (Applied Biosystems). *Septin1* (Mm00450521_m1), *septin2* (Mm00447971_m1),

septin3 (Mm00488730_m1), *septin4* (Mm00448225_m1), *septin5* (Mm01175430_m1), *septin6* (Mm00490843_m1), *septin7* (Mm00550197_m1), *septin8* (Mm01290063_m1), *septin9* (Mm01248788_m1), *septin10* (Mm00556875_m1), *septin11* (Mm01347587_m1), *septin12* (Mm01170241_m1), *septin14* (Mm01197708_m1), *cdc42ep2* (Mm0127921_m1), *cdc42ep3* (Mm04208750_m1), *cdc42ep5* (Mm00517581_m1), *cdc42ep4* (Mm01246312_m1), *cdc42ep1* (Mm00840486_m1), *Gapdh* (Mm99999915_g1).

Flow cytometry and cell sorting

Peripheral blood and BM cells were analyzed according to stranded procedures and samples were analyzed on LSR Fortessa or LSRII flow cytometry (BD Bioscience). In transplantation to distinguish donors from recipient cells by using Ly45.2 (Clone 104, eBioscience) and Ly45.1 (Clone A20, eBioscience) monoclonal antibodies. For PB and BM lineage cell analysis, we used the antibodies anti-CD3 ϵ (clone 145-2C11), anti-B220 (clone RA3-6B2), anti-Mac1 (clone M1/70), anti-Gr-1 (clone RC57BL/6-8C5), and all the antibodies from eBiosciences. For early hematopoiesis analysis, mononuclear cells were isolated by low-density centrifugation (Histopaque 1083, Sigma-Aldrich; Histopaque 1.084, GE Health Care) and stained with lineage cocktail antibodies. After that lineage depletion by magnetic separation using Dynabeads (Invitrogen) was performed. Lineage-depleted cells were stained with anti-Sca-1, PE-Cy7-conjugated (clone D7), anti-c-Kit, APC-conjugated (clone 2B8), anti-CD34, FITC-conjugated (clone RAM34), anti-Flk2, PE-conjugated (clone A2F10), anti-IL7R (clone A7R34), anti-CD16/CD32 (clone 93), and streptavidin, eFluor-450 conjugated (all antibodies from eBioscience). FACS analyses data (stem and progenitor cells) were plotted as a percentage of long-term hematopoietic stem cells (LT-HSCs, gated as LSK CD34^{-low}Flk2⁻), short-term hematopoietic stem cells (ST-HSCs, gated as LSK CD34⁺Flk2⁻), and multipotent progenitors (LMPPs, gated as LSK CD34⁺Flk2⁺) distribution among donor-derived LSKs (Lin^{neg}c-kit⁺sca-1⁺ cells). Lymphoid and myeloid progenitors are plotted as a percentage of common lymphoid progenitors (CLPs: gated as IL7R⁺ population among Lin^{neg} Sca-1^{low}c-Kit^{low} cells), common myeloid progenitors (CMPs, gated as Lin^{neg}c-kit⁺CD34⁺CD16/32⁻), megakaryocyte-erythrocyte progenitors (MEPs gated as Lin^{neg}c-kit⁺CD34⁻CD16/32⁻), and granulocyte-macrophage progenitors (GMPs gated as Lin^{neg}c-kit⁺CD34⁺CD16/32⁺). FACS analyses data (differentiated cells) are plotted as the percentage of B cells (B220⁺), T cells (CD3⁺), and myeloid (Gr-1⁺, Mac-1⁺, and Gr-1⁺Mac-1⁺) cells among donor-derived Ly5.1⁺ cells. To isolate HSCs, lineage depletion was performed to enrich for lineage negative cells, which were then stained with the above-mentioned antibodies and LT-HSCs were sorted using a BD FACS Aria III (BD Biosciences).

CASIN treatment

Aged LT-HSCs were incubated for 12–16 h with CASIN (5 μ M) at 37°C (5% CO₂, 3% O₂) in growth factors free medium and subsequently analyzed by immunofluorescence studies or analyzed by real-time RT-PCR.

Immunofluorescence staining

Freshly sorted LT-HSCs were seeded on fibronectin-coated glass coverslips. Cells were fixed with BD Cytofix Fixation Buffer (BD Biosciences). After fixation, cells were washed with PBS,

permeabilized with 0.2% Triton X-100 (Sigma) in PBS for 20 min, and blocked with 10% Donkey serum (Sigma) for 20 min. Both primary and secondary antibody incubations were performed for 1 h at room temperature. Coverslips were mounted with ProLong Gold Antifade Reagent with or without DAPI (Invitrogen, Molecular Probes). The cells were coimmunostained with an anti-alpha tubulin antibody (Abcam, rat monoclonal ab 6160); Borg4 (Santa Cruz, goat polyclonal) and Borg3 (Santa Cruz, goat polyclonal) were detected with an anti-rat and goat DyLight 488-conjugated antibody or goat Alexa Fluor 647 (Jackson Immuno Research), an anti-Cdc42 antibody (Abcam or Millipore rabbit polyclonal), anti-Cdc42-GTP antibody (mouse monoclonal), an anti-AcH4K16 antibody (Millipore, rabbit polyclonal), Septin7 (Proteintech, rabbit polyclonal), Septin6 (Santa Cruz, rabbit polyclonal), Septin2 (Santa Cruz or Abcam rabbit polyclonal) were detected with an anti-rabbit DyLight594-conjugated or cy3-conjugated antibody (Jackson Immuno Research). Samples were imaged with an Axio Observer Z1 microscope (Zeiss) equipped with a 63× PH objective. Some of the samples were analyzed with Axio scan microscope with 40× objective. Alternatively, samples were analyzed with an LSM710 confocal microscope (Zeiss) equipped with a 63× objective. Primary raw data were imported into the Volocity Software package (version 6.0, Perkin Elmer) for further processing.

Proximity ligation assay

Freshly sorted LT-HSCs were seeded on fibronectin-coated glass coverslips. Cells were fixed with BD Cytofix Fixation Buffer (BD Biosciences). After fixation, cells were gently washed with PBS, permeabilized with 0.2% Triton X-100 (Sigma) in PBS for 20 min, and blocked with 10% donkey serum (Sigma) for 20 min. To determine the Cdc42-Borg4 and Borg4-Septin7 interactions, the cells were then incubated with primary antibody mixtures Cdc42 (Millipore rabbit polyclonal) and Borg4 (Santa Cruz, goat polyclonal) and Septin7 (Proteintech, rabbit polyclonal) at room temperature for 1 h. Diluted PLA probes were mixed and incubated on the cover glass at 37°C for 1 h and followed by incubation with ligation mix for 30 min at 37°C. The amplification mix was then applied for 100 min at 37°C. The coverslips were mounted on microscope slides with Doulink mounting medium with DAPI, and the cells imaged with a LSM710 confocal microscopy. Further analyzed raw data by using Volocity Software package (version 6.0, Perkin Elmer) to get 3D images and fluorescent intensity calculations.

Competitive transplantation assays

For competitive bone marrow transplantation assays, young (10–16 weeks old) *Sept7^{fl/fl}* and *Septin7^{A/A}* or *Borg4^{fl/fl}* and *Borg4^{A/A}* mice were used as donors. A total of 1×10^6 donor BM cells were mixed with equal amount of bone marrow cells from Ly5.1⁺ BoyJ competitor mice and transplanted into lethally irradiated Ly5.1⁺ BoyJ recipient mice. Peripheral blood chimerism was determined by FACS analysis up to 21 weeks after primary transplantation. BM cells were analyzed 20–21 weeks after primary transplantation. For analysis of the function of *Septin-7* HSCs, at week 21, 2×10^6 bone marrow cells from individual primary recipient mice were injected into individual lethally irradiated secondary recipient Ly5.1⁺ BoyJ mice.

Homing assay

LSK cells (CD45.2⁺) were sorted by flow cytometry. LSK cells were cultured with CFSE at 37°C for 8 min. The reaction was then terminated with 10% FBS at 4°C for 2 min and washed two times with cold PBS. LKS⁺ cells (1×10^6) were intravenously injected into lethally irradiated (11 Gy) recipient mice (CD45.1⁺). The recipient mice were sacrificed at 16 h after transplantation. CFSE⁺ cells in BM of recipient mice were analyzed by FACS.

Single-cell proliferation assay

Single-cell proliferation assay was performed as described previously (Senger *et al*, 2017). Here, single LT-HSCs were sorted from the bone marrow of *Septin7^{fl/fl}* and *Septin7^{A/A}* mice using BD FACS Aria into the wells of Terasaki plate with culturing medium containing IMDM+ 10% FBS added with 100 ng/ml granulocyte colony-stimulating factor (G-CSF), thrombopoietin (TPO), and stem cell factor (SCF). These cells were incubated for 48 h at 37°C, 5% CO₂, and 3% O₂. Within the next 48 h, the plates were read for completed cell divisions and dead cells every 8 h. For the first division, wells were counted with two cells, second division counted with three to four individual cells.

Statistical analyses

The statistical analysis was performed within GraphPad prism 7.0. All data were plotted as mean with SD or mean with SEM as minimum and maximum points. Student *t*-test was used to access the significance difference between the means of two groups. One-way ANOVA and two-way ANOVA were used for more than three groups. Bonferroni post-test to compare all pair of dataset was determined when the overall *P* value was < 0.05.

Data availability

Primary data will be provided upon request. This study does not include data deposited in an external database.

Expanded View for this article is available online.

Acknowledgments

The authors would like to thank the flow cytometry core facility for cell sorting and for imaging confocal microscopy at Ulm University and the Tierforschungszentrum at the University of Ulm for their support. We thank the RIKEN Bioresource Center, Japan, for providing borg4 floxed embryos. A.G. was supported by the Marie Curie Ageing Network MARRIAGE funded by the EU. K.S. was supported by the RTG 1789 CEMMA funded by the DFG. R.K. was supported by the FOR 2674 funded by the DFG. Open Access funding enabled and organized by Projekt DEAL.

Author contributions

RK, KSe, and HG were involved in experimental planning and interpretation of results. RK, KSe performed experiments. AG performed confocal microscopy analysis. TS performed AxioScan microscopy for imaging. KSe performed cell sorting. VS performed transplantation experiments. KE performed real-time PCR experiments. YZ, MCF, and HG supported the

overall study design. MBM and MG provided *Septin7^{fl/fl}* mice and reviewed and edited the manuscript. RK and HG wrote and edited the manuscript.

Conflict of interest

The authors declare that they have no conflict of interest.

References

- Abbey M, Hakim C, Anand R, Lafera J, Schambach A, Kispert A, Taft MH, Kaever V, Kotlyarov A, Gaestel M *et al* (2016) GTPase domain driven dimerization of SEPT7 is dispensable for the critical role of septins in fibroblast cytokinesis. *Sci Rep* 6: 20007
- Adolfsson J, Månsson R, Buza-Vidas N, Hultquist A, Liuba K, Jensen CT, Bryder D, Yang L, Borge O-J, Thoren LAM *et al* (2005) Identification of Flt3+ lympho-myeloid stem cells lacking erythro-megakaryocytic potential a revised road map for adult blood lineage commitment. *Cell* 121: 295–306
- Ageta-Ishihara N, Yamazaki M, Konno K, Nakayama H, Abe M, Hashimoto K, Nishioka T, Kaibuchi K, Hattori S, Miyakawa T *et al* (2015) A Cdc42EP4/septin-based perisynaptic glial scaffold facilitates glutamate clearance. *Nat Commun* 6: 10090
- Akunuru S, Geiger H (2016) Aging, clonality and rejuvenation of hematopoietic stem cells. *Trends Mol Med* 22: 701–712
- Althoff MJ, Nayak RC, Hegde S, Wellendorf AM, Bohan B, Filippi M-D, Xin M, Lu QR, Geiger H, Zheng YI *et al* (2020) Yap1-Scribble polarization is required for hematopoietic stem cell division and fate. *Blood* 136: 1824–1836
- Amoah A, Keller A, Emini R, Hoenicka M, Liebold A, Vollmer A, Eiwien K, Soller K, Sakk V, Zheng YI *et al* (2021) Aging of human hematopoietic stem cells is linked to changes in Cdc42 activity. *Haematologica* <https://doi.org/10.3324/haematol.2020.269670>
- Beerman I, Maloney WJ, Weissmann IL, Rossi DJ (2010) Stem cells and the aging hematopoietic system. *Curr Opin Immunol* 22: 500–506
- Brown JL, Jaquenoud M, Gulli MP, Chant J, Peter M (1997) Novel Cdc42-binding proteins Gic1 and Gic2 control cell polarity in yeast. *Genes Dev* 11: 2972–2982
- Busch K, Klapproth K, Barile M, Flossdorf M, Holland-Letz T, Schlenner SM, Reth M, Höfer T, Rodewald H-R (2015) Fundamental properties of unperturbed haematopoiesis from stem cells *in vivo*. *Nature* 518: 542–546
- Chambers SM, Boles NC, Lin K-Y, Tierney MP, Bowman TV, Bradfute SB, Chen AJ, Merchant AA, Sirin O, Weksberg DC *et al* (2007) Hematopoietic fingerprints: an expression database of stem cells and their progeny. *Cell Stem Cell* 5: 578–591
- Chollet J, Dünkler A, Bäuerle A, Vivero-Pol L, Mulaw MA, Gronemeyer T, Johnsson N (2020) Cdc24 interacts with septins to create a positive feedback loop during bud site assembly in yeast. *J Cell Sci* 133: jcs240283
- Croker BA, Metcalf D, Robb L, Wei W, Mifsud S, DiRago L, Cluse LA, Sutherland KD, Hartley L, Williams E *et al* (2004) SOCS3 is a critical physiological negative regulator of G-CSF signaling and emergency granulopoiesis. *Immunity* 20: 153–165
- Dong F, Hao S, Zhang S, Zhu C, Cheng H, Yang Z, Hamey FK, Wang X, Gao AI, Wang F *et al* (2020) Differentiation of transplanted haematopoietic stem cells tracked by single-cell transcriptomic analysis. *Nat Cell Biol* 22: 630–639
- Eduardo da Silva L, Russo LC, Forti FL (2020) Overactivated Cdc42 acts through Cdc42EP3/Borg2 and NCK to trigger DNA damage response signaling and sensitize cells to DNA-damaging agents. *Exp Cell Res* 395: 112206
- Farrugia AJ, Calvo F (2016) The Borg family of Cdc42 effector proteins Cdc42EP1-5. *Biochem Soc Trans* 44: 1709–1716
- Farrugia AJ, Calvo F (2017) Cdc42 regulates Cdc42EP3 function in cancer-associated fibroblasts. *Small GTPases* 8: 49–57
- Farrugia AJ, Rodríguez J, Orgaz JL, Lucas M, Sanz-Moreno V, Calvo F (2020) CDC42EP5/BORG3 modulates SEPT9 to promote actomyosin function, migration, and invasion. *J Cell Biol* 219: e201912159
- Florian M, Dörr K, Niebel A, Daria D, Schrezenmeier H, Rojewski M, Filippi M-D, Hasenberg A, Gunzer M, Scharffetter-Kochanek K *et al* (2012) Cdc42 activity regulates hematopoietic stem cell aging and rejuvenation. *Cell Stem Cell* 10: 520–530
- Florian MC, Klose M, Sacma M, Jablanovic J, Knudson L, Nattamai KJ, Marka G, Vollmer A, Soller K, Sakk V *et al* (2018) Aging alters the epigenetic asymmetry of HSC division. *PLoS Biol* 16: e2003389
- Florian MC, Leins H, Gobs M, Han Y, Marka G, Soller K, Vollmer A, Sakk V, Nattamai KJ, Rayes A *et al* (2020) Inhibition of Cdc42 activity extends lifespan and decreases circulating inflammatory cytokines in aged female C57BL/6 mice. *Aging Cell* 19: e13208
- Florian MC, Nattamai KJ, Dörr K, Marka G, Überle B, Vas V, Eckl C, Andrä I, Schiemann M, Oostendorp RAJ *et al* (2013) A canonical to non-canonical Wnt signalling switch in haematopoietic stem-cell ageing. *Nature* 503: 392–396
- Geiger H, de Haan G, Florian MC (2013) The ageing haematopoietic stem cell compartment. *Nat Rev Immunol* 13: 376–389
- Geiger H, Koehler A, Gunzer M (2007) Stem cells, aging, niche, adhesion and Cdc42: a model for changes in cell-cell interactions and hematopoietic stem cell aging. *Cell Cycle* 6: 884–887
- Grigoryan A, Guidi N, Senger K, Liehr T, Soller K, Marka G, Vollmer A, Markaki Y, Leonhardt H, Buske C *et al* (2018) LaminA/C regulates epigenetic and chromatin architecture changes upon aging of hematopoietic stem cells. *Genome Biol* 19: 189
- Guidi N, Sacma M, Ständker L, Soller K, Marka G, Eiwien K, Weiss JM, Kirchhoff F, Weil T, Cancelas JA *et al* (2017) Osteopontin attenuates aging-associated phenotypes of hematopoietic stem cells. *EMBO J* 36: 840–853
- Hirsch DS, Pirone DM, Burbelo PD (2001) A new family of Cdc42 effector proteins, CEPs, function in fibroblast and epithelial cell shape changes. *J Biol Chem* 276: 875–883
- Joberty G, Perlungher RR, Macara IG (1999) The Borgs, a new family of Cdc42 and TC10 GTPase-interacting proteins. *Mol Cell Biol* 19: 6585–6597
- Joberty G, Perlungher RR, Sheffield PJ, Kinoshita M, Noda M, Haystead T, Macara IG (2001) Borg proteins control septin organization and are negatively regulated by Cdc42. *Nat Cell Biol* 3: 861–866
- Kammaing LM, de Haan G (2006) Cellular memory and hematopoietic stem cell aging. *Stem Cells* 24: 1143–1149
- Kim MS, Froese CD, Estey MP, Trimble WS (2011) SEPT9 occupies the terminal positions in septin octamers and mediates polymerization-dependent functions in abscission. *J Cell Biol* 195: 815–826
- Kinoshita M (2003) Assembly of mammalian septins. *J Biochem* 134: 491–496
- Kremer BE, Haystead T, Macara IG (2005) Mammalian septins regulate microtubule stability through interaction with the microtubule-binding protein MAP4. *Mol Biol Cell* 16: 4648–4659
- Leins H, Mulaw M, Eiwien K, Sakk V, Liang Y, Denking M, Geiger H, Schirmbeck R (2018) Aged murine hematopoietic stem cells drive aging-associated immune remodeling. *Blood* 132: 565–576
- Liu W, Du W, Shang X, Wang L, Evelyn C, Florian MC, A. Ryan M, Rayes A, Zhao X, Setchell K *et al* (2019) Rational identification of a Cdc42 inhibitor presents a new regimen for long-term hematopoietic stem cell mobilization. *Leukemia* 33: 749–761

- Low C, Macara IG (2006) Structural analysis of septin 2, 6, and 7 complexes. *J Biol Chem* 281: 30697–30706
- Mejia-Ramirez E, Florian MC (2020) Understanding intrinsic hematopoietic stem cell aging. *Haematologica* 105: 22–37
- Mejia-Ramirez E, Geiger H, Florian MC (2020) Loss of epigenetic polarity is a hallmark of hematopoietic stem cell aging. *Hum Mol Genet* 29: R248–R254
- Menon MB, Gaestel M (2015) Sep(t)arate or not – how some cells take septin-independent routes through cytokinesis. *J Cell Sci* 128: 1877–1886
- Menon MB, Sawada A, Chaturvedi A, Mishra P, Schuster-Gossler K, Galla M, Schambach A, Gossler A, Förster R, Heuser M et al (2014) Genetic deletion of SEPT7 reveals a cell type-specific role of septins in microtubule destabilization for the completion of cytokinesis. *PLoS Genet* 10: e1004558
- Mostowy S, Cossart P (2012) Septins: the fourth component of the cytoskeleton. *Nat Rev Mol Cell Biol* 13: 183–194
- Mujal AM, Gilden JK, Gérard A, Kinoshita M, Krummel MF (2016) A septin requirement differentiates autonomous and contact-facilitated T cell proliferation. *Nat Immunol* 17: 315–322
- Ni F, Yu W-M, Wang X, Fay ME, Young KM, Qiu Y, Lam WA, Sulchek TA, Cheng T, Scadden DT et al (2019) Ptpn21 Controls Hematopoietic Stem Cell Homeostasis and Biomechanics. *Cell Stem Cell* 24: 608–620
- Okada S, Leda M, Hanna J, Savage NS, Bi E, Goryachev AB (2013) Daughter cell identity emerges from the interplay of Cdc42, septins, and exocytosis. *Dev Cell* 26: 148–161
- Rossi DJ, Jamieson CHM, Weissman IL (2008) Stems cells and the pathways to aging and cancer. *Cell* 132: 681–696
- Saçma M, Pospiech J, Bogeska R, de Back W, Mallm J-P, Sakk V, Soller K, Marka G, Vollmer A, Karns R et al (2019) Haematopoietic stem cells in perisinusoidal niches are protected from ageing. *Nat Cell Biol* 21: 1309–1320
- Sadian Y, Gatsogiannis C, Patasi C, Hofnagel O, Goody RS, Farkasovský M, Raunser S (2013) The role of Cdc42 and Gic1 in the regulation of septin filament formation and dissociation. *Elife* 2: e01085
- Senger K, Marka G, Soller K, Sakk V, Florian MC, Geiger H (2017) Septin 6 regulates engraftment and lymphoid differentiation potential of murine long-term hematopoietic stem cells. *Exp Hematol* 55: 45–55
- Shcheprova Z, Baldi S, Frei SB, Gonnet G, Barral Y (2008) A mechanism for asymmetric segregation of age during yeast budding. *Nature* 454: 728–734
- Sheffield PJ, Oliver CJ, Kremer BE, Sheng S, Shao Z, Macara IG (2003) Borg/septin interactions and the assembly of mammalian septin heterodimers, trimers, and filaments. *J Biol Chem* 278: 3483–3488
- Sirajuddin M, Farkasovsky M, Hauer F, Kühlmann D, Macara IG, Weyand M, Stark H, Wittinghofer A (2007) Structural insight into filament formation by mammalian septins. *Nature* 449: 311–315
- Snoeck H-W (2013) Aging of the hematopoietic system. *Curr Opin Hematol* 20: 355–361
- Takizawa PA, DeRisi JL, Wilhelm JE, Vale RD (2000) Plasma membrane compartmentalization in yeast by messenger RNA transport and a septin diffusion barrier. *Science* 290: 341–344
- Tooley AJ, Gilden J, Jacobelli J, Beemiller P, Trimble WS, Kinoshita M, Krummel MF (2009) Amoeboid T lymphocytes require the septin cytoskeleton for cortical integrity and persistent motility. *Nat Cell Biol* 11: 17–26
- Wang J, Geiger H, Rudolph KL (2011) Immunoaging induced by hematopoietic stem cell aging. *Curr Opin Immunol* 23: 532–536



License: This is an open access article under the terms of the Creative Commons Attribution-NonCommercial-NoDerivs License, which permits use and distribution in any medium, provided the original work is properly cited, the use is non-commercial and no modifications or adaptations are made.